Molecular Biology of the Cell
Vol. 16, 2746–2758, June 2005

Microtubules Are Dispensable for the Initial Pathogenic Development but Required for Long-Distance Hyphal Growth in the Corn Smut Fungus *Ustilago maydis*

Uta Fuchs, Isabel Manns, and Gero Steinberg

Max-Planck-Institut für terrestrische Mikrobiologie, D-35043 Marburg, Germany

Submitted March 1, 2005; Revised March 31, 2005; Accepted April 1, 2005
Monitoring Editor: David Drubin

Fungal pathogenicity often involves a yeast-to-hypha transition, but the structural basis for this dimorphism is largely unknown. Here we analyze the role of the cytoskeleton in early steps of pathogenic development in the corn pathogen *Ustilago maydis*. On the plant yeast-like cells recognize each other, undergo a cell cycle arrest, and form long conjugation hyphae, which fuse and give rise to infectious filaments. F-actin is essential for polarized growth at all these stages and for cell-cell fusion. Furthermore, F-actin participates in pheromone secretion, but not perception. Although *U. maydis* contains prominent tubulin arrays, microtubules are neither required for cell-cell recognition, nor for cell-cell fusion, and have only minor roles in morphogenesis of yeast-like cells. Without microtubules hyphae are formed, albeit at 60% reduced elongation rates, but they reach only ~50 μm in length and the nucleus fails to migrate into the hypha. A similar phenotype is found in dynein mutants that have a nuclear migration defect and stop hyphal elongation at ~50 μm. These results demonstrate that microtubules are dispensable for polarized growth during morphological transition, but become essential in long-distance hyphal growth, which is probably due to their role in nuclear migration.

INTRODUCTION

Plant pathogens are an important threat to mankind, as it was estimated that they are responsible for a preharvest loss to food and cash crops of 42% of potential production on a global basis (Oerke *et al.,* 1994). Considering the increasing world population, a better understanding of the molecular basis of phytopathology and important pathogens is therefore required. Pathogenic development of many fungi requires a yeast-hyphal transition, which enables the pathogen to be passively spread or to actively invade substrates by polar hyphal growth (overview in Gow, 1995). Morphological changes during this morphological switch involve polarized growth that is thought to depend on the cytoskeleton, which provides tracks for the delivery of supplies to the expanding hyphal tip (review in Geitmann and Emons, 2000). Indeed, numerous studies demonstrate a crucial role of F-actin in polarized fungal growth (reviewed by Harold, 1990) and fungal endocytosis (reviewed in Engqvist-Goldstein and Drubin, 2003), whereas a few reports confirm the importance of F-actin in the dimorphic transition (Yokoyama *et al.,* 1990; Akashi *et al.,* 1994). In contrast, the importance of microtubules (MT) is much less clear. MTs are involved in nuclear migration (reviewed by Xiang and Fischer, 2004), but they have no obvious role in tip growth of *Candida albicans* (Yokoyama *et al.,* 1990) and *Saccharomyces cerevisiae* (Huffaker *et al.,* 1988). In contrast, disruption of MTs drastically reduced tip growth rates in *Aspergillus nidulans* (Horio and Oakley, 2005) and led to branching in *Schizosaccharomyces pombe* (Sawin and Nurse, 1998). Despite the fact that the role of MTs in plant pathogenic fungi is even less understood, the tubulin cytoskeleton is the major target for some commonly used fungicides (summarized in Holloman *et al.,* 1997), which is due to the crucial role of tubulin in mitosis. However, many fungal pests apparently do not undergo any cell division on the plant surface (Fischer and Holton, 1957; Heath and Heath, 1979), which might be due to a cell cycle arrest (Garcia-Muse *et al.,* 2003). Thus, it is an important question whether MTs have additional roles in polarized growth during pathogenic development.

During the last decade, the fungus *Ustilago maydis* became a model system for analysis of the molecular basis of fungal plant pathogenicity (Basse and Steinberg, 2004; Kahmann and Kämper, 2004). This basidiomycete belongs to the smut fungi, an important group of plant pathogens that can cause considerable grain yield loss and economic damage (Agrios, 1997). Consequently, *U. maydis* is considered to be a potential threat to the economy of North America and is listed by Ad Hoc Group of the Biological Weapons Convention (Madden and Wheelis, 2003). Recently, much progress has been made in understanding the organization of the cytoskeleton in yeast-like cells of *U. maydis* (Steinberg *et al.,* 2001; Banuett and Herskowitz, 2002; Straube *et al.,* 2003; Adamikova *et al.,* 2004). However, very little is known about the structural basis of the yeast-hyphal transition during mating, cell-cell fusion, and subsequent polarized growth of *b*-dependent hyphae. Pathogenic development of corn smut starts with the recognition of mating pheromone secreted by yeasts of the opposite mating type (reviewed in Banuett, 1995). This induces a cell-cycle arrest (Garcia-Muse *et al.,* 2003) and triggers cells to switch from their default budding program to filamentous growth, which results in the formation of long conjugation hyphae. These filaments grow toward each other and fuse at their tips. Combining the cytoplasm of compatible cells leads to the formation of the *bE/bW* tran-

This article was published online ahead of print in *MBC in Press* (http://www.molbiolcell.org/cgi/doi/10.1091/mbc.E05–03–0176) on April 13, 2005.

Address correspondence to: Gero Steinberg (Gero.Steinberg@staff.uni-marburg.de).

Table 1. Genotype of strains used in this study

Strains	Genotype	Reference
AB33	*a2 PnarbW2 PnarbE1, ble^R*	Brachmann *et al.* (2001)
AB33GT	*a2 PnarbW2 PnarbE1, ble^R/potefGFPTub1*	Manns *et al.*, unpublished results
AB33G$_3$Myo5_RT	*a2 PnarbW2 PnarbE1, ble^R/pGFP$_3$myo5/potefRFPTub1*	Manns *et al.*, unpublished results
FB2	*a2b2*	Brachmann *et al.* (2001)
FB2GT	*a2b2*/potefGFPTub1	Steinberg et al. (2001)
FB1Dyn2^{ts}	*a1b1* Δ *dyn2::dyn2^{ts}, nat^R*	Wedlich-Söldner et al 2002
FB2Peb1Y	*a2b2 peb1-yfp, ble^R*	Straube *et al.* (2003; =FBEBY)
FB1Y	*a1b1*/pOY	Weber *et al.* (2003)
FB2C	*a2b2*/pOC	Weber *et al.* (2003)
FB1mG	*a1b1*/pmfa1GFP	Spellig *et al.* (1996)
FB2mG	*a2b2*/pmfa1GFP	Spellig *et al.* (1996)
potefRFP$_2$Tub1	P*otef-2mrfp-tub1, hyg^R*	Manns *et al.*, unpublished results
pGFP$_3$Myo5C	P*myo5-3gfp-myo5, cbx^R*	Weber *et al.* (2003)
pOY	P*otef-yfp, cbx*^{R}	Weber *et al.* (2003)
pOC	P*otef-cfp, cbx*^{R}	Weber *et al.* (2003)
pmfa1GFP	P*mfa1-egfp,cbx*^{R}	Weber *et al.* (2003)

a, b, mating type loci; *mfa2*, mating pheromone 2; P, promoter; -, fusion; *ble^R*, phleomycine resistance; *cbx^R*, carboxin resistance; /, ectopically integrated; *otef*, constitutive promoter (Spellig *et al.*, 1996); *nar*, conditional nitrate reductase promoter (Banks *et al.*, 1993); *bE1*, *bW2*, genes of the *b* mating type locus; *egfp*, enhanced green fluorescent protein; *yfp*, yellow-shifted fluorescent protein; *cfp*, cyan-shifted fluorescent protein; *mfa1*, mating pheromone 1 (Bölker *et al.*, 1992); *tub1*, α-tubulin; *peb1*, EB1-homologue; *myo5*, class V myosin; *dyn2^{ts}*, temperature-sensitive allele of the C-terminal part of the dynein heavy chain.

scription factor that triggers growth of the *b*-dependent hyphae on the surface of plant epidermis and is a major regulator of the following steps in pathogenic development of *U. maydis* (reviewed in Kahmann and Kämper, 2004).

Here we set out to elucidate the role of the cytoskeleton in yeasts, pheromone-induced conjugation hyphae, cell-cell fusion in mating, and growth of *b*-dependent hyphae. We demonstrate that F-actin is essential for polarized growth in all stages and is required for cell-cell fusion. In contrast, MTs are dispensable for mating and growth of conjugation and *b*-dependent hyphae up to a length, when nuclei start to migrate into the hyphae. However, MTs become essential for extended hyphal growth and nuclear migration.

MATERIALS AND METHODS

Growth Conditions and Induction of Formation of Conjugation Hyphae and b*-dependent Hyphae*

U. maydis wild-type strain FB2 (for details of strains see Table 1) was grown over night at 28°C in complete medium (CM; Holliday, 1974) supplemented with 1% glucose (CM-G) to an OD_{600} = 0.6. Formation of conjugation hyphae was induced by the addition of 0.5 μl synthetic pheromone (pheromone; *a1* or *a2*, stock 2.5 μg/μl dimethyl sulfoxide [DMSO]), final concentration 2.5×10^{-3} μg/μl; Szabo *et al.*, 2002) to 500 μl of FB2, FB2Peb1Y cell suspension in a 2-ml reaction tube and incubation for 5–7 h at 22°C, 200 rpm. Growth of *b*-dependent filaments was monitored in strains AB33, AB33GT, and AB33GFP$_3$Myo5_RT that contain the filament-inducing *bE/bW* transcription factor under the control of the nitrate inducible *nar* promoter (Banks *et al.*, 1993). *b*-dependent filamentous growth was induced by growing cells overnight in CM-G to OD_{600} ~0.8 ×10 ml cell suspension was centrifuged at 3000 rpm for 3 min and resuspended in 10 ml nitrate minimal medium supplemented with 1% glucose (NM-G; Holliday, 1974). Cells were analyzed after 6–7 h of growth in NM-Glucose at 28°C.

Inhibitor Studies

For all inhibitor experiments with haploid yeast-like cells 500 μl cell suspension were incubated in a 2-ml reaction tube and either benomyl at 0.1–20 μM (stock 10 mM in DMSO, Sigma-Aldrich, Steinheim, Germany), latrunculin A (LatA) at 0.1–10 μM (stock 20 mM in DMSO, kindly provided by Dr. Karen Tenney, University of California, Santa Cruz) was added for 1–8 h with gentle shaking. In control experiments the corresponding amount of the solvent DMSO was used. To investigate the effect of these drugs on growth of conjugation hyphae, cells were first treated for 1.5 h with synthetic pheromone (see above) before LatA, benomyl, or DMSO was added and cells were incubated for additional 5.5 h. To investigate the role of the cytoskeleton in *b*-dependent hyphae strain AB33 was grown overnight to a cell density of OD_{600} = 0.8 in CM-G. Cells were harvested by centrifugation and resuspended in the same volume of fresh hyphal growth-inducing NM-medium and incubated at 28°C (200 rpm), after 2.5 h 500 μl cell suspension were transferred into a 2 ml reaction tube and DMSO, benomyl, or LatA at a final concentration of 0.1–10 μM was added. Cells were analyzed after additional 6–8 h at 28°C. In the subsequent quantitative analysis on the influence of benomyl on growth of *b*-dependent hyphae 8 ml of AB33 (preincubated for 2 h in NM) cell culture was incubated with 20 μM benomyl or the equivalent amount of DMSO in a culture flask at 28°C, 200 rpm. Cells were sampled every hour and cell length was measured using MetaMorph (Universal Imaging) software. To disrupt MTs in *b*-dependent hyphae of strain AB33GT 500 μl cell suspension was incubated with 10 μM benomyl or the corresponding amount of DMSO for 30 min at 28°C (200 rpm). For indirect detection of F-actin 500 μl of a suspension of AB33GFP$_3$Myo5_RT hyphae (7h NM) were treated with 100 μM carbonyl cyanide *m*-chlorophenyl-hydrazone (CCCP) for 10 min and rigorous binding of GFP-Myo5 to F-actin was immediately monitored. To confirm that these filaments are indeed F-actin, cell were incubated in 50 μM LatA for 30 min, subsequently treated with 100 μM CCCP for 10 min, and microscopically analyzed.

Mating on Water Agar and Confrontation Assays

The ability to undergo cell fusion was assayed on 2% water agar. Fifty microliters of water agar, supplemented with either 20 μM benomyl, 50 μM LatA, or the equal amount of DMSO, were placed on a coverslip and kept in a wet chamber until use. Strains FB1YFP and FB2CFP that express cytoplasmic YFP or CFP, respectively, were grown to a density of OD_{600} = 0.8, centrifuged at 3000 rpm for 3 min, and concentrated to a final cell density of OD_{600} = 5.0. Two milliliters of each cell suspension were combined and incubated for 1 h at room temperature at 150 rpm. Subsequently, 3 μl of the cell mixture was placed on top of the water agar droplet and slides were incubated in a moist chamber for 13, 17, and 25 h at 22°C. Cell fusion was analyzed by detecting CFP and YFP signals. Structures that contained both fluorescent proteins were counted as products derived from fusion of two cells, whereas cells with only CFP or YFP signals were considered to be single. Confrontation assays were performed as described by Snetselaar *et al.* (1996). In brief, slides were covered with 200 μl of 2% water agar, containing either 20 μM benomyl, 50 μM LatA, or the equal amount of the solvent DMSO. Strains FB1mG and FB2mG that contain GFP under the control of the pheromone-sensitive *mfa1*-promoter (Spellig *et al.*, 1996) were grown to a cell density of OD_{600} = 0.8, centrifuged at 3000 rpm, and concentrated to OD_{600} = 5. One microliter of each cell suspension was placed confronting the other on the water agar film in a distance of ~200 μm or less. Confrontation assays were covered with 1 μl of paraffin oil and incubated in a moist chamber for 16–22 h at 22°C.

Stimulation with Synthetic Pheromone to Assay Pheromone Perception

For pheromone stimulation strain FB1mG that contains GFP under the control of the pheromone-sensitive *mfa1*-promoter (Spellig *et al.*, 1996) was grown to a cell density of OD_{600} = 0.5. 500 μl cell suspension was supplemented with DMSO as control, 50 μM LatA for 1 h at 22°C, horizontally shaking at 200 rpm. Subsequently 0.5 μl of synthetic pheromone (*a2*, stock 2.5 ng/μl DMSO; Szabo *et al.*, 2002) was added and cells were incubated in a 2-ml Eppendorf tube for 2 h at 200 rpm, 22°C. Finally, GFP expression as a read out for pheromone perception was monitored microscopically.

Nuclear Staining with DAPI

For 4,6-diamidino-2-phenylindole (DAPI; Sigma-Aldrich; D-9542) staining of nuclei in conjugation hyphae, FB2 cells were first stimulated with synthetic pheromone. After 1.5 h of incubation 20 μM benomyl or the equal volume of DMSO was added to the cells. For the same experiment $Dyn2^{ts}$ cells were pheromone stimulated as described above and after 3 h of incubation at 22°C were shifted to permissive growth temperature, 32°C. Samples were taken after 4 and 7 h of incubation. Cells were fixed with 3% formaldehyde for 10 min, washed in phosphate-buffered saline (PBS) twice, and resuspended in ~50 μl ddH_2O. Samples were mounted on poly-L-lysine cover slips incubated for 3 min and dried at 60°C. Coverslips with fixed cells were washed in PBS several times and stained with DAPI (0.5 μg/ml) for 10 min at 60°C. Coverslips were washed several times in PBS before analysis.

Microscopy, Image Processing, and Quantitative Analysis

Cells from logarithmically growing cultures were dropped on a thin 2% agarose-layer and immediately observed using a Zeiss Axioplan II microscope (Carl Zeiss, Oberkochen, Germany). Epifluorescence of GFP was observed using standard FITC filters. For colocalization studies, YFP and CFP were analyzed with specific filter sets (YFP: BP500/20, FT515, BP535/30; CFP: BP436, FT455, BP480–500). Frames were taken with a cooled CCD-camera (CoolSNAP HQ, Photometrics, Tucson, AZ) that was controlled by the MetaMorph (Universal Imaging, West Chester, PA) software. Measurements and image processing, including adjustment of brightness, contrast, and gamma-values were performed with MetaMorph (Universal Imaging) and Photoshop (Adobe, San Jose, CA). To determine the length of hyphae, the distance between the tip of the hyphae and the mother cell (excluding the mother cell) was measured; in case of the bipolar growing hyphae only the length of the longer filament was determined.

Statistical analysis by two-tailed *t* test at $\alpha = 0.05$ was carried out using Prism (GraphPad, San Diego, CA). All values are given as means ± SD unless otherwise stated.

RESULTS

b-*dependent Hyphae of* U. maydis *Contain Cytoskeletal Tracks*

The current model for hyphal growth assumes that MTs are tracks for long-distance traffic, whereas F-actin supports short-range motility of membranous organelles within the hyphal apex (Steinberg, 2000). To visualize MTs in hyphae we expressed GFP-α tubulin in strain AB33 (AB33GT), which grows filamentously upon shift to nitrate containing medium. The resulting *b*-dependent hyphae contain long MTs that reach into the hyphal apex and the basal septum that separates the empty parts of the growing hyphae from the living tip cell (Figure 1, arrow). Unfortunately, all attempts to visualize F-actin filaments including staining with rhodamine–phalloidin and expression of GFP-tropomyosin failed in *U. maydis*. However, treatment of a strain that expressed GFP-myosin 5 ($AB33GFP_3Myo5\_RT$) with 100 μM carbonyl cyanide *m*-chlorophenyl-hydrazone (CCCP), an uncoupler of the oxidative chain that rapidly depletes ATP from the cytosol (Azarkina and Konstantinov, 2002) led to the appearance of GFP-Myo5–bound filaments that were sensitive to 50 μM of the actin inhibitor LatA (Figure 1B), suggesting that they are F-actin cables. The existence of both MTs and F-actin cables in hyphal cells confirm previous results on yeast-like cells (Steinberg *et al.*, 2001; Banuett and Herskowitz, 2002), indicating that both cytoskeletal elements participate in morphogenesis and polar growth in the various developmental stages of *U. maydis.*

Morphology of Yeast-like Cells and Hyphae Depends on F-actin

In the presence of the solvent DMSO the cigar-shaped yeast-like cells of *U. maydis* grew normally with polar budding (Figure 2, control). In contrast, LatA, which most likely specifically disrupts F-actin (Spector *et al.*, 1989; Ayscough *et al.*, 1997), inhibited bud growth and affected the shape of the cell (Figure 2A; LatA). Interestingly, in the presence of LatA both daughter as well as older mother cells changed shape and swelled, indicating that the older cell walls are still flexible. Benomyl, 20 μM, disrupted MTs in these cells (Straube *et al.*, 2003) and led to an accumulation of large budded cells (Figure 2, C1, Benomyl) that contained condensed nuclei within the mother cell (unpublished data), indicating that benomyl treatment arrests cells in mitosis. In addition, extended incubation also resulted in ~5% cells that showed lateral budding (up to 2.5%) or grew bipolar or slightly irregular (Fig: 2, C2), indicating that MTs have a role in morphogenesis and polarity of haploid cells. A quantitative analysis of these effects revealed that yeast-like cells are highly sensitive to LatA treatment, because half of the cells showed aberrant growth and morphology at ~1–1.5 μM LatA (IC_{50}: ~1.3 μM). In comparison, cells were able to tolerate up to 1 μM benomyl (IC_{50}: ~1.0 μM) before the number of arrested cells increased.

Microtubules Are Dispensable for Conjugation Tube Formation

On treatment with synthetic pheromone yeast-like cells undergo a cell cycle arrest and form long conjugation hyphae that, under normal conditions, search for the compatible mating partner (Figure 3A). In the presence of 10 μM LatA cells do not form these hyphae and do not show any signs of hyphal growth (Figure 3B). Interestingly, conjugation hyphae formation was highly sensitive to LatA, as no hyphae were found at concentrations above 0.1 μM (Figure 3E). In contrast, disruption of MTs by up to 20 μM benomyl did not abolish conjugation tube formation, although these hyphae were shorter and occasionally branched (Figure 3C, arrows). To confirm that the drug disrupts MTs in conjugation hyphae, we treated pheromone-stimulated cells of strain FB2GT with benomyl. Indeed, the inhibitor efficiently disrupted GFP-labeled MTs in those conjugation hyphae (Figure 3D). Therefore our results demonstrated that MTs are not essential for growth of conjugation hyphae.

Microtubules Are Required for Long-distance Hyphal Growth

On the plant surface two compatible mating hyphae grow toward each other and fuse eventually. This allows the assembly of a heterodimeric *bE/bW* transcription factor that induces extended filamentous growth in order to infect the host tissue (Banuett, 1995). We made use of strain AB33 (Brachmann *et al.*, 2001) in order to investigate the role of the cytoskeleton in infective *b*-dependent hyphae. This strain contains both parts of the *bE/bW* transcription factor under the control of the nitrate inducible *nar* promoter (Banks *et al.*, 1993). On shift to nitrate containing medium AB33 cells start to form straight hyphae until the living tip cell leaves behind empty sections at the subapical region (Figure 4A, control, arrow) that are thought to allow *b*-dependent hyphae to grow on the plant surface without access to nutrients (Steinberg *et al.*, 1998). Consistent with the results on yeast-like cells and conjugation hyphae, treatment with 10 μM LatA impaired growth of *b*-dependent hyphae (Figure 4B, LatA). Growth inhibition was already seen at very low amounts of

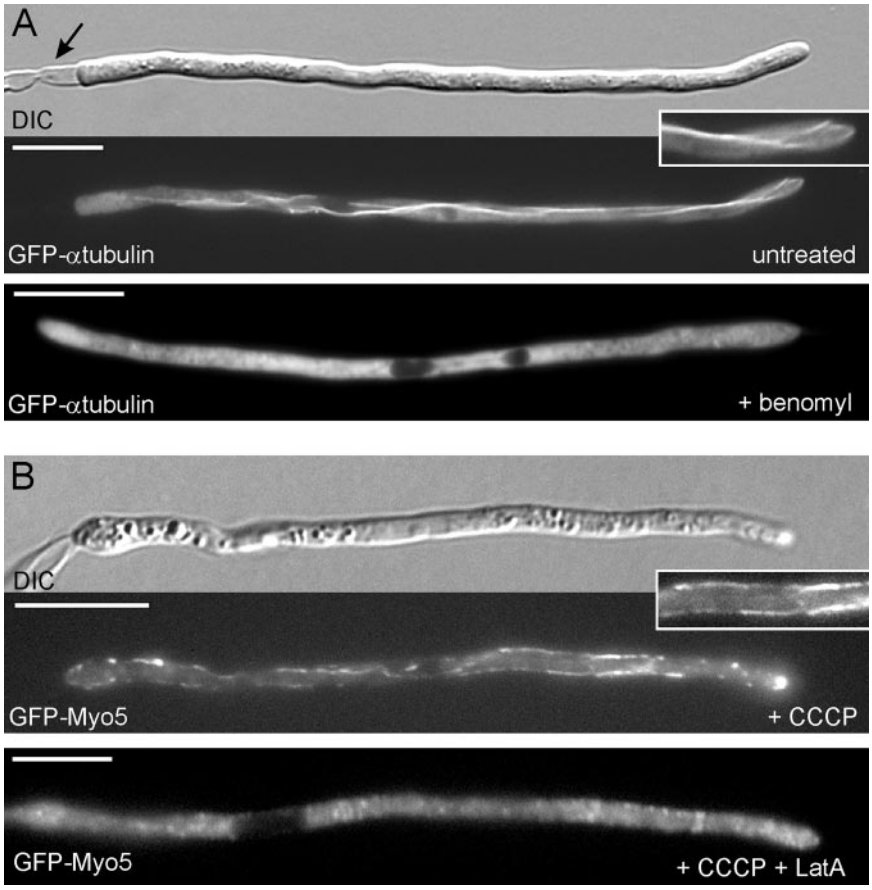

Figure 1. The effect of inhibitors on the cytoskeleton in *b*-dependent hyphae. (A) Infectious hyphae of *U. maydis* consist of an elongated tip cell that leaves behind empty sections (arrow) in order to grow for long distances on the surface of the plant, where no nutrients are accessible. Long microtubules reach into the hyphal apex that are sensitive to treatment with 10–20 μM benomyl for 30 min. Note that only cytoplasmic background of depolymerized GFP-α tubulin is visible. Bar, 10 μm. (B) Previous studies have demonstrated that hyphal growth depends on a class V myosin, Myo5 (Weber *et al.,* 2003). Myo5 localizes to filamentous structures in the presence of 100 μM CCCP, which decouples the oxidative chain, thereby lowering the cellular ATP levels. These myosin-bound filaments are sensitive to treatment with 50 μM latrunculin A (LatA), suggesting that they are F-actin. Bar, 10 μm.

LatA (IC_{50}: ~0.1 μM) (Figure 4D). However, in the presence of LatA ~20% of the cells were slightly elongated (Figure 4B), which might be due to that fact that hyphal growth of AB33 cells was induced for 2.5 h in drug-free medium, before LatA was applied. In contrast, treatment with 20 μM benomyl did not abolish growth of *b*-dependent hyphae (Figure 4C, Ben). However, in the absence of MTs hyphae grew irregular and often at both cell poles (Figure 4C, Ben, arrowheads). More strikingly, benomyl-treated hyphae remained shorter than control hyphae (Figure 4C, benomyl). In addition, without MTs empty sections were not formed, but the apices of older hyphae were often filled with vacuoles (Figure 4C, benomyl, inset).

These results indicated that shorter *b*-dependent hyphae are formed in the absence of MTs. It was recently described that disruption of MTs significantly slowed down the growth rate of *A. nidulans* hyphae (Horio and Oakley, 2004). Therefore, we considered it possible that the shorter hyphae of benomyl treated cells in *U. maydis* are also a consequence of reduced tip growth rates and that long *b*-dependent hyphae are formed after extended growth in nitrate-containing medium. Indeed, quantitative analysis of hyphal growth velocities in the presence of the solvent DMSO (Figure 5A, control) and 20 μM benomyl (Figure 5A, benomyl) revealed that disruption of MTs lowered the elongation rates by ~60% (control: 8.23 ± 0.49 μm/h; benomyl: 3.61 ± 0.40 μm/h). However, even after >14 h of growth in benomyl, *b*-dependent hyphae remained shorter (Figure 5B, + ben, ON), indicating that MTs are required for growth of *b*-dependent hyphae above 50–60 μm. Interestingly, a similar result was found in conjugation hyphae. These hyphae only rarely formed empty sections but reach up to 100 μm in length (Figure 5B). Again, in the presence of benomyl conjugation hyphae remained shorter (Figure 5B) and reach a maximum length of ~50 μm.

Defects in Long-distance Hyphal Growth Coincide with Impaired Nuclear Migration

We next asked why MTs become essential for filamentous growth in longer conjugation hyphae. In control hyphae nuclei are positioned 50.2 ± 7.8 μm (n = 23 conjugation hyphae) behind the growing tip (Figure 5C, control; DAPI-stained nuclei indicated by asterisk) and 90% of wild-type hyphae (35–60 μm in length, n = 20 hyphae) contained a nucleus in the hypha. In the presence of 20 μM benomyl in 82% of all cells the nucleus remained in the mother cell, whereas hyphae were formed at one or both cell poles (Figure 5C, arrows; nuclei indicated by asterisk). We consid-

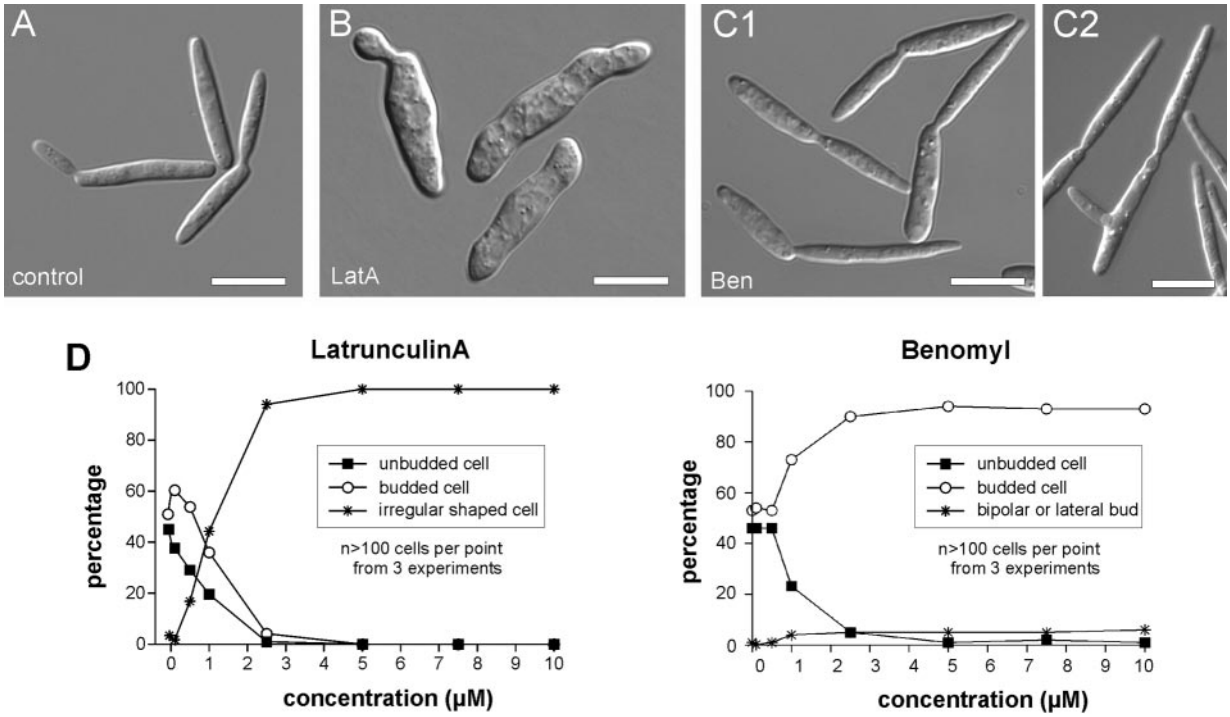

Figure 2. F-actin and microtubules in morphogenesis of haploid yeast-like cells. (A) Yeast-like cells are elongated and grow by polar budding (control). (B) Disruption of F-actin by 20 μM latrunculin A (LatA) impaired polar bud formation and led to irregular and swollen cells, indicating that actin-based transport is essential for morphogenesis of the yeast-like cells. (C1) Six hours of treatment with 20 μM of the microtubule inhibitor benomyl (Ben) resulted in disruption of MTs (Straube *et al.*, 2003) and led to an accumulation of large budded cells that contained condensed nuclei (unpublished data), suggesting that cells are arrested in mitosis. (C2) In addition, cells apparently were not arrested but showed morphological defects, including lateral budding and slight alterations in cell shape. Bars: 10 μm. (D) Treatment of nonsynchronized cultures of yeast-like cells with increasing amounts of inhibitors revealed that the cells are highly sensitive to latrunculin A (IC_{50}: ~1.3 μM), whereas they can cope with up to 1 μM benomyl before large budded and morphologically aberrant cells accumulate (IC_{50}: ~1.0 μM). Treatment with higher concentrations of benomyl led to ~90% cells arrested in mitosis, whereas the rest showed slight defects in cell shape or lateral budding, indicating that MTs have multiple roles in the yeast stage.

ered it possible that this defect in nuclear migration underlies the growth inhibition of MT-deficient hyphae. To gain further support for this notion, we made use of a conditional dynein mutant that is defective in nuclear migration (Straube *et al.*, 2001; Wedlich-Söldner *et al.*, 2002). In pheromone-induced conjugation hyphae of strain FB2Peb1Y, plus-end binding Peb1-YFP moves to the apex in 83.5 ± 5.0 cases (n = 2 experiments, 27 hyphae), indicating that conjugation hyphae also focus their MT plus-ends toward the growing hyphal tip (Figure 5D). Consequently, pheromone-treated dynein mutants formed hyphae. However, nuclei never migrated into the hyphae and tip growth also stopped at ~50 μm length (Figure 5, C and B; Dyn2ts), whereas cells formed new hyphae at the opposite cell pole (Figure 5C; Dyn2ts, arrow marks bipolar hyphae, asterisk indicates nucleus). Interestingly, the length of dynein mutant hyphae also did not exceed a length of 45 ± 8.97 μm (n = 30) when incubated overnight (Figure 5B, Dyn2ts ON). This phenotype of dynein mutant hyphae was remarkably similar to that of benomyl-treated cells. Therefore, we consider it possible that hyphal elongation beyond 50–60 μm requires nuclear migration in order to maintain communication between the nucleus and the expanding hyphal tip.

F-actin Participates in Pheromone Secretion but not in Perception

We finally set out to analyze the role of the cytoskeleton in the perception of pheromone. We made use of strain FB1mG that expresses GFP under the control of the mating pheromone *a*-promoter (*mfa*). This promoter is induced shortly after recognition of compatible pheromone, which allows monitoring of pheromone perception by analyzing GFP expression (Spellig *et al.*, 1996). Under natural conditions cells have to recognize a pheromone gradient that is produced by the compatible mating partner. This situation is given in confrontation assays, where compatible strains are placed on water agar facing each other and are overlaid by paraffin oil that allows diffusion of secreted pheromone (Snetselaar *et al.*, 1996). Indeed, in these assays FB1mG and FB2mG cells recognized each other, which is indicated by *mfa1*-promoter driven GFP expression, and formed long conjugation hyphae that bridge the gap between both strains (Figure 6A). In the presence of benomyl both strains were stimulated, but only short conjugation hyphae were formed (Figure 6B, inset). Consistent with the results described above these hyphae did not elongate any further (Figure 6B, compare inset at 16 and 22 h), but were able to bridge smaller gaps between the compatible strains (Figure 6B, right panel). In contrast, disruption of F-actin by 50 μM LatA not only abolished filament formation but also impaired pheromone perception in these assays (Figure 6C). Interestingly, the ability to perceive pheromone was dependent on the distance between the partners, with strong GFP expression when compatible cells were in very close contact (Figure 6C). This indicated that F-actin was required to percept very low amounts of secreted pheromone. To test this hypothesis,

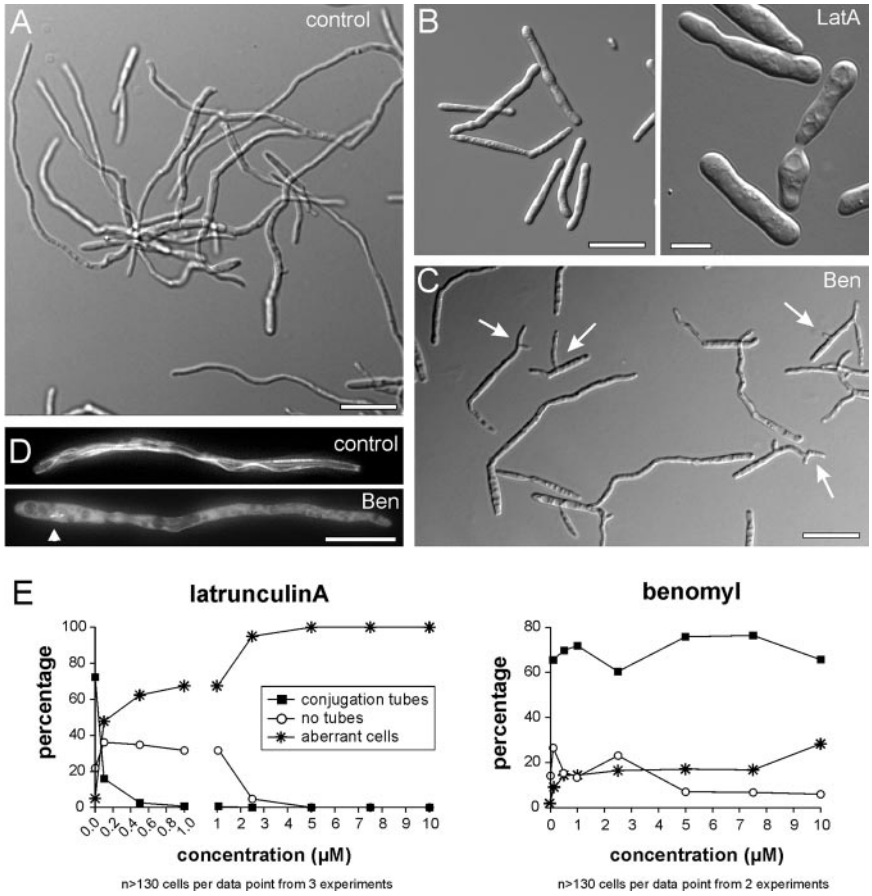

Figure 3. F-actin and microtubules in growth of conjugation hyphae. (A) On treatment of yeast-like cells with synthetic pheromone for 8 h, long conjugation hyphae are formed that, under natural conditions, would fuse with a compatible cell in order to form a *b*-dependent hypha. Bar, 20 μm. (B) Treatment of cells that were preincubated with pheromone for 1.5 h with 5 μM latrunculin A for a further 6.5 h completely abolished hyphal growth. Even at higher magnification no signs of tube formation was found. Bars, 20 μm (left image) and 5 μm (right image). (C) Even after 8 h in 20 μM benomyl (cells were preincubated with pheromone for 1.5 h before addition of benomyl) cells formed conjugation tubes that were shorter and occasionally branched (arrows). Bar, 20 μm. (D) Benomyl (10 μM, 30 min) indeed disrupts microtubules that reach into the tip of conjugation hyphae. Only MT fragments were occasionally found (arrowhead). Bar, 10 μm. (E) Quantitative analysis of the effect of cytoskeleton inhibitors revealed that tube formation is very sensitive against disruption of F-actin (IC_{50}: <0.1 μM), whereas benomyl treatment had almost no effect, suggesting that microtubule-based transport is dispensable for growth of conjugation hyphae. However, a stable portion of ~10–30% branched hyphae appeared, indicating that MTs participate in cell polarity of hyphal tip cells.

we incubated liquid cell cultures with synthetic pheromone. At a pheromone concentration of 2.5 ng/μl >95% of both LatA- and DMSO-treated cells showed GFP expression, confirming that F-actin is not essential for pheromone perception at high concentrations (Figure 6E). However, cells treated with highly diluted synthetic pheromone (Figure 6E; 2.5 and 1×10^{-2} ng) in the presence of DMSO and LatA showed comparable levels of pheromone stimulation. At this low concentration only 20–40% of the control cells were stimulated (Figure 6E). This argues against a need of F-actin for perception of pheromone traces. Alternatively, we considered it possible that LatA-treated cells are defective in pheromone secretion, which would also result in reduced perception and, consequently, less GFP expression in confrontation assays.

Cell-Cell Fusion Requires F-actin but not Microtubules

Our data demonstrate that shorter conjugation hyphae are formed in the absence of MTs, whereas F-actin is crucial at this stage. This suggested that short MT-independent conjugation hyphae confer cell-cell fusion. We therefore developed an assay that allowed the quantitative analysis of fusion of compatible cells that express either CFP or YFP. When plated on water agar strain FB1Y and FB2C recognized each other and started to form conjugation hyphae that grew toward the mating partner (Figure 7A; in overlay CFP in red, YFP in green). After ~7 h mating partners occasionally found each other and the tips of the conjugation hyphae were curled around the compatible partner cell (Figure 7B; arrow), whereas the older parts of the cell became vacuolated (Figure 7B; arrowheads). These structures contain both CFP and YFP (Figure 7B, overlay in yellow), demonstrating that both compatible cells fused and mixed their cytoplasm. However, in order to circumvent the initial steps of cell-cell recognition, we incubated compatible strains at high density (OD_{600} = 5) in liquid culture for 1 h. Under these conditions, strains FB1mG and FB2mG that express GFP as a result of pheromone recognition (Spellig *et al.*, 1996) are stimulated but do not show conjugation tube formation (Figure 7C). After similar pretreatment of strains

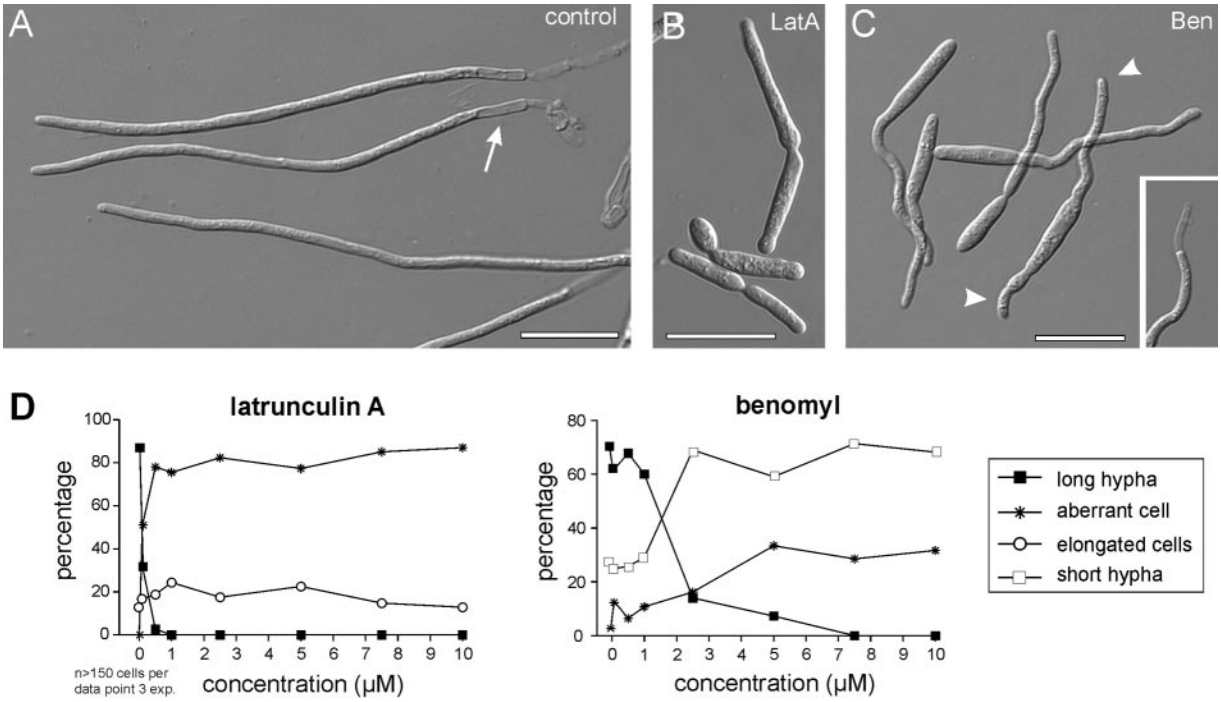

Figure 4. F-actin and microtubules in growth of *b*-dependent hyphae. (A) Under natural conditions compatible mating partners provide the two parts of the heterodimeric transcription factor bE/bW that triggers formation of a *b*-dependent dikaryotic hypha (Banuett, 1995). Strain AB33 contains both *b* genes under the control of the *nar* promoter that is induced upon shift to nitrate-containing medium, which results in filamentous growth (Brachmann *et al.*, 2001), control). Similar to the dikaryotic *b*-dependent hyphae on the plant surface, this induced *b*-dependent filament grows by tip extension and forms empty sections (control, arrow). (B) In the presence of 5 μM latrunculin A only very few elongated cells were formed (LatA), and most cells remained in their yeast-like stage. (C) In the presence of 10 μM benomyl cells occasionally show multiple budding, but also form filaments. However, these filaments remain shorter, and empty parts were often formed at the tip of hyphae (inset). Bars, 20 μm. (D) Hyphal growth was extremely sensitive to disruption of F-actin by latrunculin A ($IC_{50} \ll 0.1$ μM). In contrast, *b*-dependent hyphae tolerated low amounts of benomyl, but the number of long hyphae that formed empty sections dramatically decreased at a concentration higher than 1.5 μM. However, most cells were able to form short hyphae in the presence of benomyl, whereas a significant portion grew bipolar or was branched (aberrant).

FB1Y and FB2C cells were plated on water agar supplemented with cytoskeletal inhibitors. This assay allowed us to monitor the need of MTs and F-actin for cell-cell fusion. Thirteen hours after incubation, cells that either contained YFP (Figure 7D, control, green) or CFP (Figure 7D, control, red) were found. In addition, *b*-dependent hyphae were seen that contained both YFP and CFP (Figure 7D, control, yellow). Fusion products were also found in the presence of 20 μM benomyl (Figure 7D, yellow, arrow), although the resulting hyphae remained shorter and grew irregularly. In contrast, in the presence of LatA no structures containing both CFP and YFP were detected, indicating that F-actin is essential for cell-cell fusion. The portion of fused cells increased over time in both DMSO- (Figure 7E, control; Figure 7F) and benomyl-treated cells (Figure 7E, benomyl, and 7F), whereas no fusion was found in LatA-treated cells. This demonstrates that F-actin is essential for this important step in the pathogenic development, whereas MTs are without detectable role in cell-cell fusion.

DISCUSSION

Many pathogenic fungi undergo a yeast-hyphal transition in order to spread within their host or to invade tissue or substrate (reviewed in Gow, 1995). The cytoskeleton is thought to be involved, but not much is known about its role in fungal dimorphism. Therefore, we have performed quantitative and qualitative studies, using specific inhibitors of F-actin and MTs, on all critical steps of the dimorphism in the plant pathogen *U. maydis.* This includes the morphogenesis of yeast-like and hyphal cells, pheromone perception and secretion, and cell-cell fusion. We demonstrate that F-actin is essential in all stages, whereas MTs are only required for long-distance growth of hyphae (Figure 8).

F-actin Is Crucial for Morphogenesis of Yeast-like Cells and Hyphae

On pheromone recognition *U. maydis* yeast-like cells switch and turn into conjugation hyphae that fuse to form a dikaryotic filament (reviewed in Banuett, 1995; Kahmann and Kämper, 2004). We found that F-actin is of key importance in all these steps. In fungi, actin exists as cortical patches and filaments (Harold, 1990; Heath, 1995), and it is thought that filaments deliver wall vesicles to the expanding growth region (Harold, 1990; Ayscough *et al.*, 1997). This notion is supported by the finding that myosin-V, which is known to be a processive organelle motor in other systems (Langford, 2002), participates in filamentous growth of *U. maydis* (Weber *et al.*, 2003). Interestingly, in *S. cerevisiae* it was reported that actin cables are not essential for the formation of mating projections, whereas cortical actin patches are crucial (Read *et al.*, 1992). Actin patches might be sites of endocytosis (reviewed in Engqvist-Goldstein and Drubin, 2003), and endocytosis also participates in polar hyphal growth of *U.*

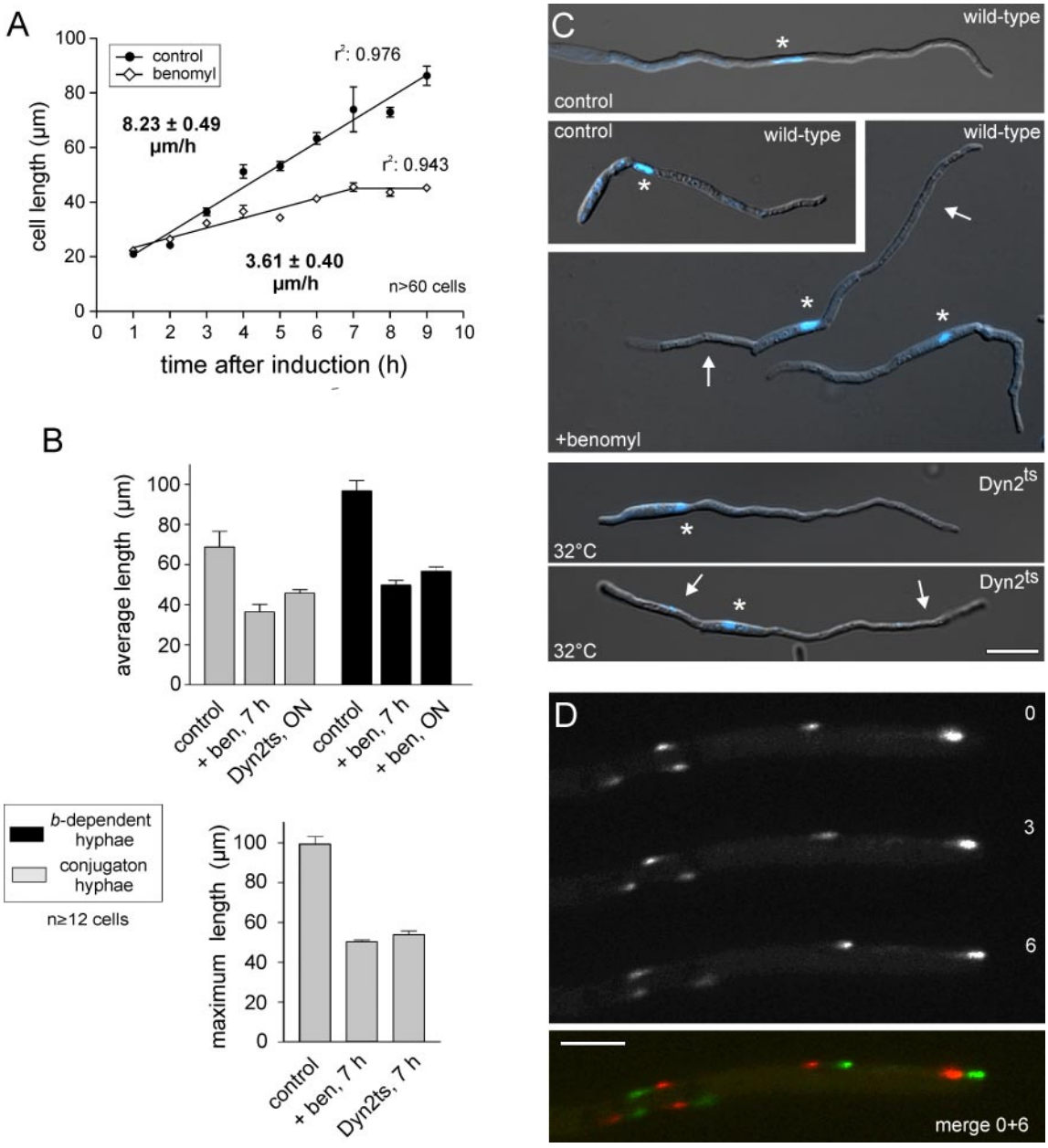

Figure 5. Growth kinetics of *b*-dependent filaments. (A) A quantitative analysis of the length of filaments over time in the presence of nitrate-containing medium supplemented with either DMSO or 20 μM benomyl revealed that MT-independent filamentous growth is significantly slower (3.61 μm/h, compared with 8.23 μm/h in untreated hyphae). (B) In the absence of MTs both conjugation and *b*-dependent hyphae are on average significantly shorter than control hyphae. Even after overnight incubation the filaments did not increase in length (+ ben, ON). In control experiments conjugation hyphae were able to reach a maximum length of 100–120 μm after 7 h (lower graph). Without MT conjugation hyphae reached a maximum hyphal length of ~60–65 μm. These results again indicate that microtubules are dispensable for short hyphal growth, but become crucial when hyphae reach ~50–60 μm in length. A temperature-sensitive dynein mutant also shows reduced growth of conjugation hyphae that reach up to ~50–60 μm length at restrictive temperatures (lower graph) and do not exceed an average length of 45.78 ± 8.97 after overnight incubation (Dyn2ts ON). (C) In pheromone-induced conjugation, hyphae nuclei are positioned near to the growing tip (control; wild-type strain FB2). Nuclear migration into the hypha starts at ~30 μm hyphal length (lower panel, control, wild-type strain FB2; nucleus indicated by asterisk). After disruption of MTs by benomyl cells grow bipolar (+benomyl, arrows; wild-type strain FB2) and nuclei remain in the mother cell (asterisk). A similar nuclear migration and growth defect was found in dynein mutants at restrictive temperature (32°C, Dyn2ts; strain FB1Dyn2^{ts}), indicating that impaired nuclear migration might underlie the tip growth defect. Bars, 10 μm. (D) Orientation of the MT plus-ends is visualized using a fusion protein of YFP and Peb1, an EB1-like MT plus-end binding protein (Straube *et al.*, 2003). In conjugation hyphae MT plus-ends carrying Peb1-YFP elongate toward the growing hyphal tip. Images are taken at three different time points (0, 3 and 6, elapsed time is given in seconds) and show the movement of the Peb1-YFP that marks MT plus-ends. The overlay of two images at T: 0s (red) and T: 6s (green) illustrates the dynamic behavior of Peb1-YFP. This orientation of MTs suggests that minus-end–directed dynein is not required for hyphal extension. Bar, 3 μm.

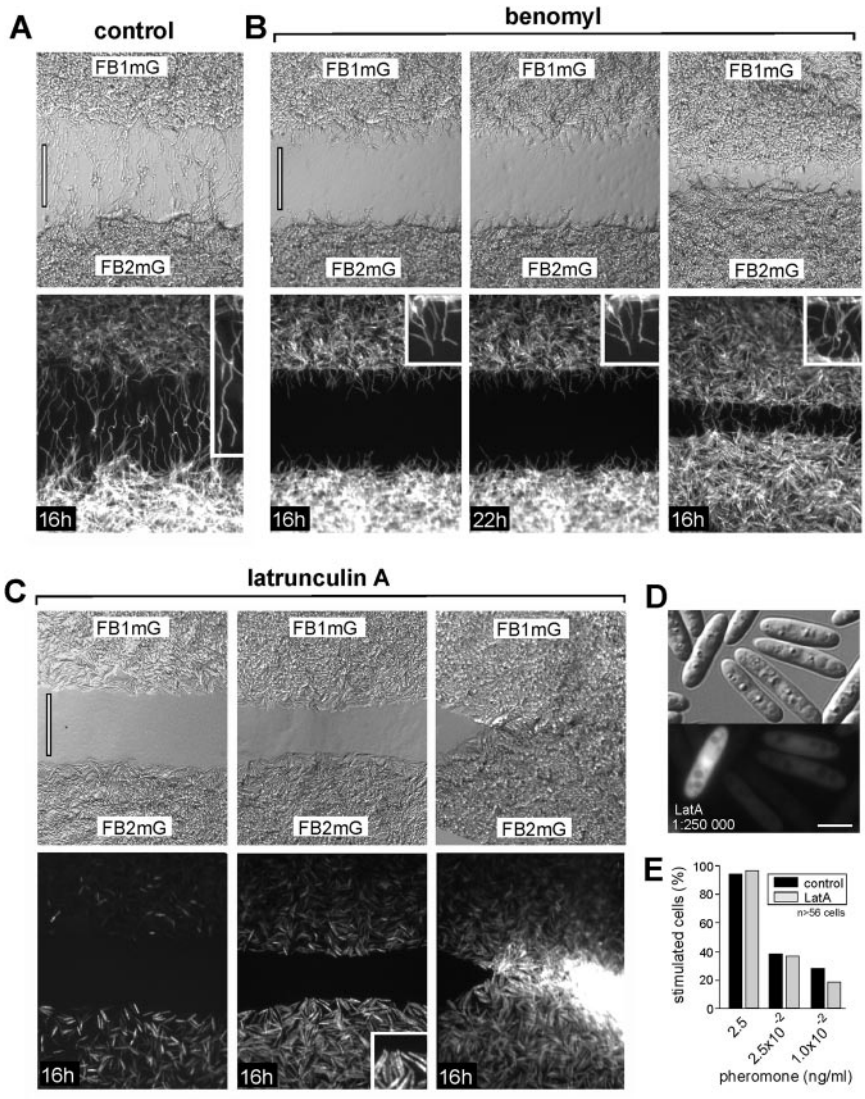

Figure 6. The cytoskeleton in recognition of the compatible mating partner. (A) In confrontation assays compatible strains that express GFP under the control of the *mfa1*-promoter were placed ~150–200 μm apart. Both strains secrete pheromone that diffuses to the compatible partner cell and induces GFP expression (lower image, 16 h after plating) and formation of long conjugation hyphae (inset). Bar, 160 μm. (B) After 16 h in the presence of benomyl only short conjugation hyphae are formed (inset), whereas pheromone perception, indicated by GFP expression, was not impaired. After additional 6 h the conjugation hyphae did not elongate any further (inset, 22 h; compare with inset at 16 h). Placing both partners close to each other allows those conjugation hyphae to bridge the distance and most likely leads to cell fusion (see Figure 7). Bar, 100 μm. (C) After disruption of F-actin no filamentous growth was detected. Surprisingly, cells were defective in pheromone perception (indicated by low GFP-expression). However, GFP-expression increased when cells were placed in closer distance to the mating partner, and strong induction of GFP expression was found when compatible cells were in close proximity. This indicates that F-actin might be essential for perception at very low pheromone concentration. Bar, 100 μm. (D) In liquid culture a dilution of pheromone (1×10^{-2} ng/μl) drastically reduced the number of cells that reacted on pheromone and decreased GFP expression. Reduced pheromone perception was detected in control strains (unpublished data) and in the presence of 50 μM latrunculin A. Bar, 5 μm. (E) Dilution of pheromone reduced the number of stimulated cells (indicated by GFP expression) in both control cells as well as latrunculin-treated cells. Note that this argues against a role of F-actin in pheromone perception at very low pheromone concentration (see Figure 6D).

maydis (Wedlich-Söldner *et al.*, 2000). Consequently, LatA-treatment might inhibit both cable-based exocytosis, as well as patch-dependent endocytosis, and this could explain why F-actin is of crucial importance in *U. maydis*. In this respect it is worth to notice that our evidence for actin cables in *U. maydis* hyphae is circumstantial. However, F-actin cables exist in yeast-like cells (Banuett and Herskowitz, 2002) and the decoration of filaments with myosin under low ATP conditions make the existence of F-actin cables likely.

The Actin Cytoskeleton Is Important for Pheromone-based Cell-Cell Communication

In confrontation assays the induction of *mfa* promoter-driven GFP expression indicated that control cells are able to detect the secreted pheromone over a distance of more than 150 μm. Under similar conditions LatA treatment abolished GFP expression, but the mating partner was recognized at shorter distances. In *S. cerevisiae* LatA treatment resulted in reduced pheromone recognition, which is thought to be due

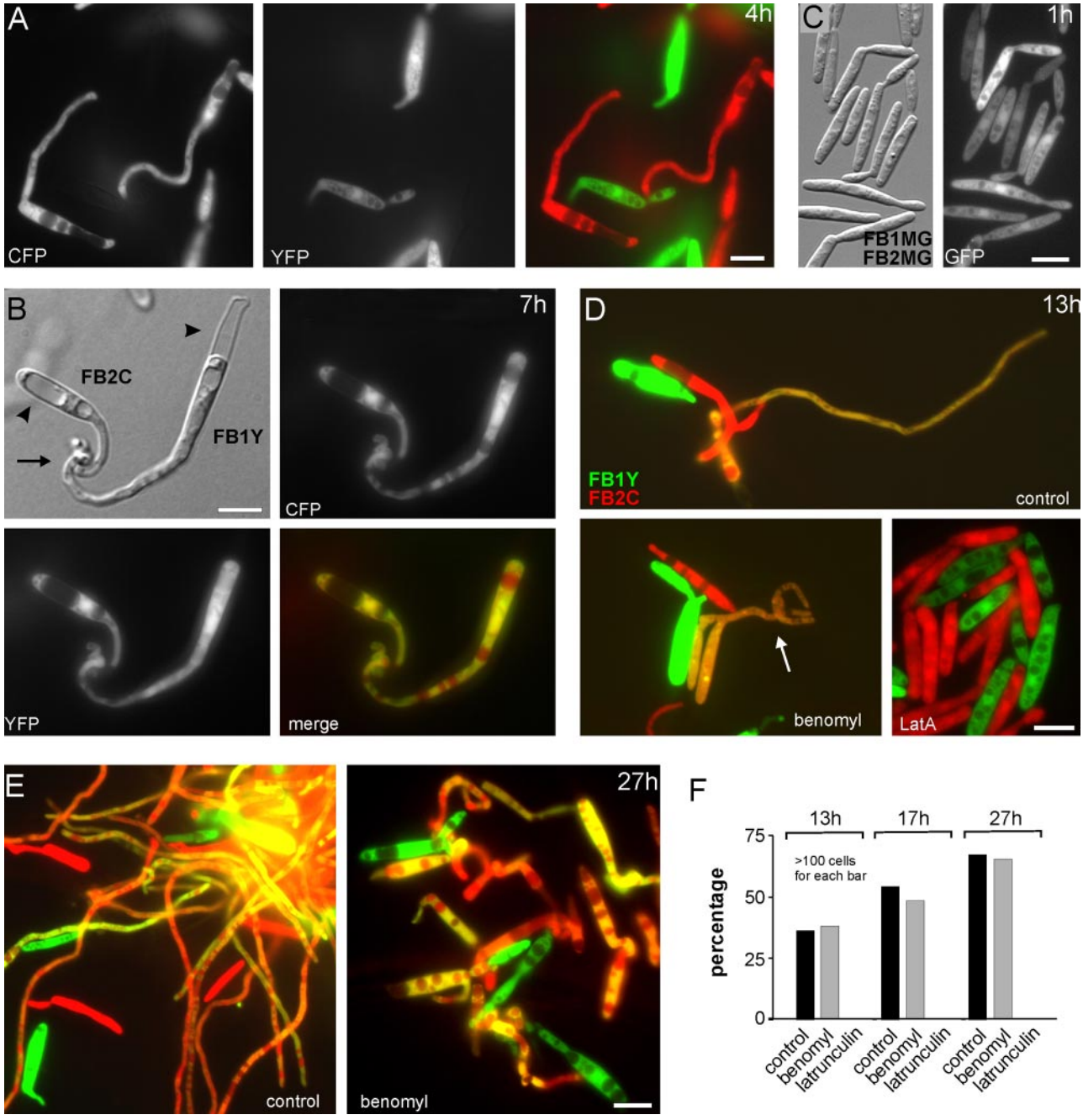

Figure 7. Quantitative analysis of the cytoskeleton in cell-cell fusion. (A) On agar compatible cells that can be identified by the expression of either CFP (strain FB1Y) or YFP (FB2C, see Table 1 for details on strains). After 4 h cells formed long conjugation hyphae that reach toward the compatible mating partner. Bar, 5 μm. (B) After 7 h conjugation hyphae reached each other, and cell fusion occurred indicated by the presence of both CFP and YFP expression in the cytoplasm (yellow in overlay). Bar, 5 μm. (C) After 1 h in suspension compatible cells at high density (OD_{600} = 5) were able to stimulate each other and induce the *mfa*-promoter–dependent expression of GFP (Spellig *et al.*, 1996), indicating that even in liquid medium the initial steps of pathogenic development are induced. Note that these cells did not yet show formation of conjugation hyphae. (D) In compatible control cells that were preincubated for 1 h at high density and subsequently placed on DMSO-containing agar (control) many cells either contained CFP or YFP, whereas about most extended filaments contained both fluorescent proteins, indicating that they are derived from cell fusion. In the presence of 20 μM benomyl cells were able to fuse, but the resulting *b*-dependent hyphae were shorter and often grew irregularly (benomyl, arrow). In the presence of 50 μM latrunculin (LatA) no cell fusion was detected. Bar, 5 μm. (E) After extended time on agar (27 h) the number of cell-cell fusions and resulting *b*-dependent hyphae increased in control experiments and under benomyl treatment, whereas no cell fusion was detected in the presence of latrunculin A (unpublished data). Note that no long hyphae are formed in the absence of microtubules. Bar, 5 μm. (F) Quantitative analysis of the presence of either CFP or YFP or both proteins in a cell reveals that cell-cell fusion is not impaired in the absence of microtubules. In contrast, F-actin is essential for cell-cell fusion. Note that this is not due to an initial defect in pheromone perception, because cells were preincubated without latrunculin A in order to allow the early recognition steps.

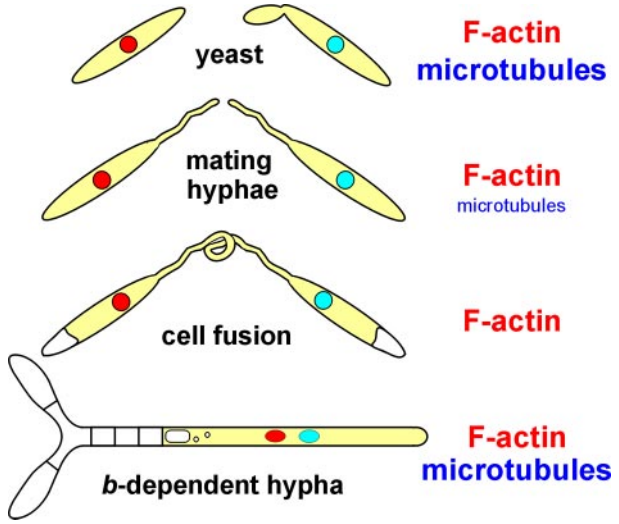

Figure 8. The role of the cytoskeleton in the morphological transition of *U. maydis*. In this study we have focused on four developmental stages in the early pathogenic development. Our data indicate that F-actin is essential in the yeast stage and is required for conjugation tube formation. Moreover, neither cell fusion nor formation of *b*-dependent hyphae was found in the absence of F-actin. Microtubules are essential in mitosis and have a role in polar growth of the bud. However, they are only of minor importance for conjugation hyphae and are dispensable for cell-cell fusion. Interestingly, MTs are also of minor importance for the formation of short *b*-dependent hyphae, but become crucial in filaments that are longer than 50–60 μm, indicating that they participate in long-distance traffic to the growing hyphal tip. Importance is indicated by size of name. Note that the role of the cytoskeleton in pheromone perception is not depicted.

to a mislocalization of the pheromone receptor (Ayscough and Drubin, 1998). However, we applied synthetic pheromone to liquid cultures at various concentrations, but could not find any reduction in the reaction to pheromone due to F-actin disruption. In confrontation assays, as well as under natural conditions on the plant surface cells have to secrete their own pheromone. This raises the possibility that LatA-treated cells might be defective in pheromone secretion, which in turn results in less perception in the partner cell. Actin-dependent exocytosis of pheromone has been described for *S. cerevisiae* (reviewed in Kurjan, 1992), and our results argue for a similar situation in *U. maydis*.

MTs Do Not Participate in Cell-Cell Fusion

In this manuscript we demonstrate that cell-cell fusion in *U. maydis* depends on intact F-actin, whereas MTs are not involved in this process. In contrast, MTs are important for cell-cell fusion in the fission yeast *S. pombe* (Petersen *et al.*, 1998). This is surprising, as both fission yeast and *U. maydis* contain prominent MT arrays (Hagan, 1998; Steinberg *et al.*, 2001) that are expected to participate in similar processes. It was speculated that the need for MTs in mating is due to MT-based transport of unknown components toward the projection tip (Petersen *et al.*, 1998). Alternatively it was suggested that the effect of MTs on cell-cell fusion could be indirect via defects in the actin cytoskeleton (Petersen *et al.*, 1998). We have preliminary evidence that benomyl treatment has no long-term effect on actin patch organization and actin cables (our own unpublished results), which might explain why *U. maydis* MTs are not involved in cell-cell fusion.

Defects in MT-based Nuclear Migration Might Be Responsible for impaired Hyphal Growth

In the absence of MTs hyphal growth in *U. maydis* continues at a rate of ~3.6 μm/h. Interestingly, in *A. nidulans* disruption of the tubulin cytoskeleton reduced the elongation velocity 10-fold to a rate of ~3.2 μm/h (Horio and Oakley, 2005), a velocity that is surprisingly similar to that of benomyl-treated *U. maydis* hyphae. Thus, slow hyphal growth of both fungi might be mediated by similar mechanisms that could involve actin-dependent myosins. Indeed, it was shown that class V myosins participate in polarized hyphal growth in *U. maydis* (Weber *et al.*, 2003) and preliminary evidence exists for a cooperation of the MT- and actin-based transport machinery in hyphal growth (I. Manns and G. Steinberg, unpublished results). Unexpectedly, MT-independent growth ceased at a hyphal length of ~50–60 μm. In control hyphae, this is exactly the distance between the nucleus and the tip, suggesting that nuclear migration and tip growth are linked. Conditional mutants in the *Ustilago* dynein have defects in nuclear migration in yeast-like cells (Straube *et al.*, 2001) and hyphae (this study), but the minus-directed dynein is most likely not directly involved in tip-growth, as the MT plus-ends are directed to the hyphal tip. Nevertheless, hyphal growth of dynein mutants also stopped at ~50–60 μm length, again supporting the notion that nuclear migration is required for extended hyphal growth. Such a connection was found in tip-growing root hairs in *A. thaliana* (Ketelaar *et al.*, 2002) and might also underlie the growth inhibition of *Aspergillus* mutants defective in NUDF, a dynein regulator that has highest homology with the human LIS1 gene (Xiang *et al.*, 1995). Furthermore, LIS1-mediated nuclear migration might be essential for neuronal cell migration and brain development (Morris *et al.*, 1998), indicating that the role of MTs in nuclear migration is of general importance in long-distance growth and migration of eukaryotic cells.

The Microtubule Cytoskeleton as a Target for Fungicides?

The actin cytoskeleton performs essential roles in all early steps of pathogenic development of *U. maydis*. Thus, any compound that interferes with the organization or function of F-actin should efficiently inhibit fungal infections. However, to our knowledge no currently used fungicide addresses components of the actin cytoskeleton, which might be due to the high degree of conservation in eukaryotic actins. On the other hand, actin-associated proteins, such as fungal specific myosin-chitin synthase fusion proteins are known to play essential roles in fungal pathogenicity (Madrid *et al.*, 2003; Liu *et al.*, 2004) and therefore might be potential targets for novel fungicides. In contrast to actin, microtubules are affected by numerous benzimidazole and phenylcarbamate fungicides (overview in Hollomon *et al.*, 1997), which might be due to their essential roles in fungal mitosis. However, good indication exists that important plant pathogens, including *U. maydis* arrest their cell cycle during early infection steps (Garcia-Muse *et al.*, 2003). In *Uromyces phaseoli* and *U. maydis* infectious hyphae consist of a single tip cell that leaves behind vacuolated parts while growing on the plant surface (Heath and Heath, 1979; Steinberg *et al.*, 1998). Thus, in these fungi anti-tubulin fungicides are expected to interfere with MTs in hyphal growth, rather than targeting mitotic events. We demonstrate here that MTs have nonessential roles in early hyphal growth, but they are essential for extended hyphal elongation, which is due to their role in nuclear migration. Therefore, anti-tubulin drugs

are expected to be ineffective in early infection, but are supposed to inhibit the infection at later stages.

ACKNOWLEDGMENTS

We thank the Deutsche Forschungsgemeinschaft for financial support (DFG SP1111).

REFERENCES

Adamikova, L., Straube, A., Schulz, I., and Steinberg, G. (2004). Calcium signaling is involved in dynein-dependent microtubule organization. Mol. Biol. Cell *15*, 1969–1980.

Agrios, G. N. (1997). Plant Pathology, London, United Kingdom: Academic Press.

Akashi, T., Kanbe, T., and Tanaka, K. (1994). The role of the cytoskeleton in the polarized growth of the germ tube in *Candida albicans*. Microbiology *140*(Pt 2), 271–280.

Ayscough, K. R., and Drubin, D. G. (1998). A role for the yeast actin cytoskeleton in pheromone receptor clustering and signalling. Curr. Biol. *8*, 927–930.

Ayscough, K. R., Stryker, J., Pokala, N., Sanders, M., Crews, P., and Drubin, D. G. (1997). High rates of actin filament turnover in budding yeast and roles for actin in establishment and maintenance of cell polarity revealed using the actin inhibitor latrunculin-A. J. Cell Biol. *137*, 399–416.

Azarkina, N., and Konstantinov, A. A. (2002). Stimulation of menaquinone-dependent electron transfer in the respiratory chain of *Bacillus subtilis* by membrane energization. J. Bacteriol. *184*, 5339–5347.

Banks, G. R., Shelton, P. A., Kanuga, N., Holden, D. W., and Spanos, A. (1993). The *Ustilago maydis nar* 1 gene encoding nitrate reductase activity: sequence and transcriptional regulation. Gene *131*, 69–78.

Banuett, F. (1995). Genetics of *Ustilago maydis*, a fungal pathogen that induces tumors in maize. Annu. Rev. Genet. *29*, 179–208.

Banuett, F., and Herskowitz, I. (2002). Bud morphogenesis and the actin and microtubule cytoskeletons during budding in the corn smut fungus, *Ustilago maydis*. Fungal Genet. Biol. *37*, 149–170.

Brachmann, A., Weinzierl, G., Kämper, J., and Kahmann, R. (2001). Identification of genes in the bW/bE regulatory cascade in *Ustilago maydis*. Mol. Microbiol. *42*, 1047–1063.

Basse, C. and Steinberg, G. (2004). *Ustilago maydis*, a model system for analysis of the molecular basis of fungal pathogenicity. Mol. Plant Pathol. *4*, 83–92.

Engqvist-Goldstein, A. E., and Drubin, D. G. (2003). Actin assembly and endocytosis: from yeast to mammals. Annu. Rev. Cell Dev. Biol. *19*, 287–332.

Fischer, G. W., and Holton, C. S. (1957): Biology and control of the smut fungi. New York: Ronald Press Company.

Garcia-Muse, T., Steinberg, G., and Perez-Martin, J. (2003). Pheromone-induced G2 arrest in the phytopathogenic fungus *Ustilago maydis*. Eukaryot. Cell *2*, 494–500.

Geitmann, A., and Emons, A. M. (2000). The cytoskeleton in plant and fungal cell tip growth. J. Microsc. *198*(Pt 3), 218–245.

Gow, N. A. (1995b). Yeast-hyphal dimorphism. In: The Growing Fungus, ed. N. A. Gow and G. M. Gadd, London: Chapman and Hall, 403–422.

Hagan, I. M. (1998). The fission yeast microtubule cytoskeleton. J. Cell Sci. *111*(Pt 12), 1603–1612.

Harold, F. M. (1990). To shape a cell: an inquiry into the causes of morphogenesis of microorganisms. Microbiol. Rev. *54*, 381–431.

Heath, I. B. (1995). The cytoskeleton. In: The Growing Fungus, ed. N.A.R. Gow and G. M. Gadd, New York: Chapman & Hall, 99–134.

Heath, I. B., and Heath, M. C. (1979). Structural studies of the development of infection structures of cowpea rust, *Uromyces phaseoli* var. *vignae*. II. Vacuoles. Can. J. Botany *57*, 1830–1837.

Holliday, R. (1974). *Ustilago maydis*. In: Handbook of Genetics, ed. R. C. King, New York: Plenum Press, 575–595.

Holloman, D. W., Butters, J. A., and Barker, H. (1997). Tubulins: a target for anti-fungal agents. In: Anti-infectives: Recent Advances in Chemistry and Structure Activity Relationships, ed. P. H. Bentley, and P. J. O'Hanlon, London, United Kingdom: Royal Society of Chemistry, 152–156.

Horio, T., and Oakley, B. R. (2005). The role of microtubules in rapid hyphal tip growth of *Aspergillus nidulans*. Mol. Biol. Cell *16*, 918–926.

Huffaker, T. C., Thomas, J. H., and Botstein, D. (1988). Diverse effects of beta-tubulin mutations on microtubule formation and function. J. Cell Biol. *106*, 1997–2010.

Kahmann, R., and Kämper, J. (2004). *Ustilago maydis*: how its biology relates to pathogenic development. New Phytol. *164*, 31–42.

Ketelaar, T., Faivre-Moskalenko, C., Esseling, J. J., de Ruijter, N. C., Grierson, C. S., Dogterom, M., and Emons, A. M. (2002). Positioning of nuclei in *Arabidopsis* root hairs: an actin-regulated process of tip growth. Plant Cell *14*, 2941–2955.

Kurjan, J. (1992). Pheromone response in yeast. Annu. Rev. Biochem. *61*, 1097–1129.

Langford, G. M. (2002). Myosin-V, a versatile motor for short-range vesicle transport. Traffic *3*, 859–865.

Liu, H., Kauffman, S., Becker, J. M., and Szaniszlo, P. J. (2004). *Wangiella* (*Exophiala*) *dermatitidis* WdChs5p, a class V chitin synthase, is essential for sustained cell growth at temperature of infection. Eukaryot. Cell *3*, 40–51.

Madden, L. V., and Wheelis, M. (2003). The threat of plant pathogens as weapons against U.S. corps. Annu. Rev. Phytopathol. *41*, 155–176.

Madrid, M. P., Di Pietro, A., and Roncero, M. I. (2003). Class V chitin synthase determines pathogenesis in the vascular wilt fungus *Fusarium oxysporum* and mediates resistance to plant defence compounds. Mol. Microbiol. *47*, 257–266.

Morris, N. R., Efimov, V. P., and Xiang, X. (1998). Nuclear migration, nucleokinesis and lissencephaly. Trends Cell Biol. *8*, 467–470.

Oerke, E. C., Dehne, H. W., Schonbeck, F., and Weber, A. (1994). Crop Production and Crop Protection: Estimated Losses in major Food and Cash Crops, New York: Elsevier.

Petersen, J., Heitz, M. J., and Hagan, I. M. (1998). Conjugation in *S. pombe*: identification of a microtubule-organising centre, a requirement for microtubules and a role for *Mad2*. Curr. Biol. *8*, 963–966.

Read, E. B., Okamura, H. H., and Drubin, D. G. (1992). Actin- and tubulin-dependent functions during *Saccharomyces cerevisiae* mating projection formation. Mol. Biol. Cell *3*, 429–444.

Sawin, K. E., and Nurse, P. (1998). Regulation of cell polarity by microtubules in fission yeast. J. Cell Biol. *142*, 457–471.

Snetselaar, K. M., Bölker, M., and Kahmann, R. (1996). *Ustilago maydis* mating hyphae orient their growth toward pheromone sources. Fungal Genet. Biol. *20*, 299–312.

Spector, I., Shochet, N., Blasberger, D., and Kashman, Y. (1989). Latrunculins novel marine macrolides that disrupt microfilament organization and affect cell growth: 1. Comparison with cytochalasin D. Cell Motil. Cytoskeleton *13*, 127–144.

Spellig, T., Bottin, A., and Kahmann, R. (1996). Green fluorescent protein (GFP) as a new vital marker in the phytopathogenic fungus *Ustilago maydis*. Mol. Gen. Genet. *252*, 503–509.

Steinberg, G. (2000). The cellular roles of molecular motors in fungi. Trends Microbiol. *8*, 162–168.

Steinberg, G., Schliwa, M., Lehmler, C., Bölker, M., Kahmann, R., and McIntosh, J. R. (1998). Kinesin from the plant pathogenic fungus *Ustilago maydis* is involved in vacuole formation and cytoplasmic migration. J. Cell Sci. *111*(Pt 15), 2235–2246.

Steinberg, G., Wedlich-Söldner, R., Brill, M., and Schulz, I. (2001). Microtubules in the fungal pathogen *Ustilago maydis* are highly dynamic and determine cell polarity. J. Cell Sci. *114*, 609–622.

Straube, A., Brill, M., Oakley, B. R., Horio, T., and Steinberg, G. (2003). Microtubule organization requires cell cycle-dependent nucleation at dispersed cytoplasmic sites: polar and perinuclear microtubule organizing centers in the plant pathogen *Ustilago maydis*. Mol. Biol. Cell *14*, 642–657.

Straube, A., Enard, W., Berner, A., Wedlich-Söldner, R., Kahmann, R., and Steinberg, G. (2001). A split motor domain in a cytoplasmic dynein. EMBO J. *20*, 5091–5100.

Szabo, Z., Tonnis, M., Kessler, H., and Feldbrügge, M. (2002). Structure-function analysis of lipopeptide pheromones from the plant pathogen *Ustilago maydis*. Mol. Genet. Genom. *268*, 362–370.

Weber, I., Gruber, C., and Steinberg, G. (2003). A class-V myosin required for mating, hyphal growth, and pathogenicity in the dimorphic plant pathogen *Ustilago maydis*. Plant Cell *15*, 2826–2842.

Wedlich-Söldner, R., Bolker, M., Kahmann, R., and Steinberg, G. (2000). A

putative endosomal t-SNARE links exo- and endocytosis in the phytopathogenic fungus *Ustilago maydis.* EMBO J. *19*, 1974–1986.

Wedlich-Söldner, R., Schulz, I., Straube, A., and Steinberg, G. (2002). Dynein supports motility of endoplasmic reticulum in the fungus *Ustilago maydis.* Mol. Biol. Cell *13*, 965–977.

Xiang, X., and Fischer, R. (2004). Nuclear migration and positioning in filamentous fungi. Fungal Genet. Biol. *41*, 411–419.

Xiang, X., Osmani, A. H., Osmani, S. A., Xin, M., and Morris, N. R. (1995). *NudF*, a nuclear migration gene in *Aspergillus nidulans*, is similar to the human *LIS-1* gene required for neuronal migration. Mol. Biol. Cell *6*, 297–310.

Yokoyama, K., Kaji, H., Nishimura, K., and Miyaji, M. (1990). The role of microfilaments and microtubules in apical growth and dimorphism of *Candida albicans.* J. Gen. Microbiol. *136*(Pt 6), 1067–1075.

Abbreviations used: MT, microtubule; F-actin, filamentous actin; GFP, green fluorescent protein; CFP, cyan-shifted fluorescent protein; YFP, yellow-shifted fluorescent protein; aa, amino acids.